Time-Dependent Behavior of Reinforced Concrete Columns Subjected to High Sustained Loads

Wenchen Ma[1]; Ying Tian, M.ASCE[2]; Hailong Zhao[3]; Sarah L. Orton, M.ASCE[4]

[1]Formerly, Ph.D. student, Dept. of Civil and Environmental Engineering and Construction, Univ. of Nevada, Las Vegas, NV 89154. E-mail: maw2@unlv.nevada.edu

[2]Professor, Dept. of Civil and Environmental Engineering and Construction, Univ. of Nevada, Las Vegas, NV 89154 (corresponding author). E-mail: ying.tian@unlv.edu

[3]Associate Professor, School of Civil Engineering, Tianjin University, Tianjin 300350, China; Formerly, Visiting Scholar, Dept. of Civil and Environmental Engineering and Construction, Univ. of Nevada, Las Vegas, NV 89154. E-mail: zhaohailong@tju.edu.cn

[4]Associate Professor, Dept. of Civil and Environmental Engineering, Univ. of Missouri, Columbia, MO 65211. Email: ortons@missouri.edu

Abstract: Several catastrophic progressive collapses of reinforced concrete buildings, initiated by column failures, occurred in the past under sustained gravity loads long after the initial construction. To study the near-failure behavior of aged concrete columns under sustained high stresses and the effects of column transverse reinforcement on nonlinear creep, thirteen columns were tested after 200 days of concrete casting. Test variables included sustained load level, age at loading, eccentricity ratio, and transverse reinforcement ratio. Two plain concrete and five reinforced concrete columns were subjected to sustained concentric loads ranging from 76% to 110% of nominal short-time strength that neglects the confinement effects provided by transverse reinforcement. One plain concrete column, as a control specimen, was also tested under concentric loading to failure in a short time. Five reinforced concrete columns were tested under sustained eccentric loading that initially caused the bending moment at the critical section to reach 77% to 100% of nominal flexural capacity. The aged columns showed high resistance to heavy sustained loads; however, one concentrically loaded and one eccentrically loaded column failed under the sustained loads. Higher column transverse reinforcement ratio decreased

concrete creep during the early stage of concentric loading and increased flexural stiffness during sustained eccentric loading, thereby reducing the risk of failure due to second order effects. Moreover, the tests indicated that Poisson's ratio of the cover concrete at the extreme compressive fibers is a suitable indicator of high sustained load levels.

Author keywords: Creep; Frame; Poisson's ratio; Progressive collapse; Reinforced concrete column; Sustained loading

Introduction

Well-engineered reinforced concrete (RC) buildings generally have a good performance. However, faulty design, overloading, construction error, poor material quality, and material deterioration do occur. Each circumstance, if not remedied timely, can lead to high stresses sustained in the concrete of RC columns as compared with their actual capacity. Once the columns fail, a progressive collapse may result. The Hotel New World, a 6-story RC frame building in Singapore, collapsed in 1986 mainly due to faulty column design (Thean et al. 1987). Persistent cracks, announcing imminent structural failure, appeared in three columns several days before the disaster. In the same year, a second-floor column failed in a 26-story RC frame apartment building in Brazil, causing a partial collapse after five hours; five days later, another partial collapse followed (Guimarães and Silva 2001). Combined design and construction mistakes were blamed for the collapse. Recently in 2021, the Champlain Towers South in Florida, U.S., a 13-story RC flat-plate apartment building, experienced a massive progressive collapse; although the exact cause of collapse is still being investigated, one or more lower-story columns failed prior to the collapse of the upper stories of the building according to a surveillance video footage. In each of these failure cases, the structure has been in years of service and, over a relatively long time period prior to the disaster, the gravity loads acting on the structure changed little. Thus, the initial failures were caused by the high stresses sustaining in RC structural components.

Sustained high stresses in concrete lead to nonlinear creep and even failure when the material suffers tertiary creep characterized by accelerated permanent strains. Accordingly, Rüsch (1960) suggested the long-term compressive strength of concrete to be 80% of its short-time strength. Concrete creep, a complex material property, is affected by a wide range of parameters. The experiments of concrete materials subjected to sustained high stresses were rare and performed predominantly within 90 days after specimen fabrication. For instance, Shah and Chandra (1970), Awad and Hilsdorf (1971), Smadi et al. (1987), and Iravani and MacGregor (1998) tested concrete cylinders or prisms subjected to sustained stresses of 60% to 95% of short-time strength; the concrete age at the beginning of sustained loading, t_0, was between 7 to 90 days. Rüsch (1960) and Stöckl (1972) reported long-term loading tests of concrete prisms, some of which were loaded at t_0 greater than 170 days; however, detailed test data such as aggregate type and creep deformation history were not provided.

Due to the use of longitudinal and transverse reinforcement, RC columns behave differently from plain concrete under sustained loads. Surprisingly, virtually no experiment data exists for RC columns under high sustained concentric loads close to their short-time capacity. It can be expected that the strain compatibility between steel and concrete causes a stress redistribution; as a result, the load carried by concrete decreases with time. Moreover, the transverse reinforcement may restrain the development and propagation of microcracks in concrete under sustained high compressive stresses, thereby delaying concrete creep and creep-induced failure; such an effect, however, has not been examined experimentally. For the design of RC tied columns under pure axial loading, ACI 318 (ACI 2019) limits the load applied on a column to 80% of its nominal axial loading capacity defined with a concrete stress of $0.85f_c'$, where f_c' is concrete short-time cylinder compressive strength. Historically, the 80% limit was used to consider both accidental eccentricity and reduced concrete strength under high sustained loads; however, since the 2014 version, ACI 318 design codes removed the intention of using this limit to address the detrimental effects of high sustained loads.

The past studies of RC columns under sustained loading focused mainly on eccentric loading response, in which concrete creep generates second order effects on column deflection and thus extra bending moment. Viest et al. (1956) conducted sustained loading tests on nineteen RC columns constructed with loading capitals. The slenderness (length-to-depth) ratio λ of the column prism portion was only 4. Jenkins and Frosch (2015) tested four RC columns with $\lambda = 12$. Other experiments reported in English literature (Green and Breen 1969 and 1984; Goyal and Jackson 1971; Khalil et al. 2001; Jenkins and Frosch 2015), however, are concerned with the creep stability of slender RC columns with λ ranging from 15 to as high as 62. Similar to the concrete material tests, the RC column tests considering high sustained loads were conducted predominantly within 3 months of concrete casting. Exceptions included two columns with $\lambda = 4$ and a high reinforcement ratio of 3% tested by Viest et al. (1956) at $t_0 = 271$ and 274 days. For the design of RC slender columns under eccentric loading, ACI 318 (ACI 2019) employs a single factor of β_{dns} as an allowance for creep-induced bending moment. This parameter, existing in the ACI 318 codes for decades, is crude because it does not take into account the various parameters affecting concrete creep.

The exact mechanism of collapse evolution of RC frame buildings under sustained gravity loading condition is largely unknown. Prior to its creep-induced failure, a column should have interacted with the surrounding elements due to the statically indeterminate nature of the structural system. Once the column fails, load redistribution can lead to high sustained stress in the nearby columns, putting them also at the risk of failure. It is not clear how high sustained stresses lead to a local column failure or how the local failure evolves into a collapse. Describing this complex time-dependent process is challenging and requires reliable structural models involving not only strength but also stiffness degradation properties. Creep of concrete under high stresses is associated with the progression of microcracks (Shah and Chandra 1970). A few nonlinear creep models (Mazzotti and Savoia 2003; Tasevski et al. 2018) have been proposed for plain concrete. These models, however, need extensive validations and did not account for the confinement effects of column transverse reinforcement on restraining concrete microcracking.

As part of an effort exploring the time-dependent near-collapse response of RC buildings overstressed by gravity loads, the experimental study presented in this paper investigated the performance of concrete columns subjected to sustained loads exceeding 75% of their short-time capacity. The tests also examined the effects of column transverse reinforcement on creep behavior and the suitability of using Poisson's ratio of concrete cover as a warning indicator of sustained high stresses in RC columns approaching failure. The study created experimental data crucial for calibrating constitutive models of concrete under sustained high stresses suitable for system-scale numerical simulations.

Test Specimens

Eight short columns under concentric loading and five longer columns under eccentric loading were tested. Specimen geometry and reinforcing details are shown in Figs. 1 and 2 for the concentrically and eccentrically loaded columns, respectively. The specimens represented the columns in a prototype RC frame building where gravity loads govern structural design. These columns contain less longitudinal reinforcement than the lower floors and are thus more prone to creep-induced failure under high sustained loads. Large-scale structural testing is preferred but it is challenging to maintain high sustained axial loads. Accordingly, the largest column section size in the sustained loading tests conducted by Viest et al. (1956), Green and Breen (1969), and Jenkins and Frosch (2015) was 152-mm square. The test specimens in this study were constructed at 1/2-scale with a 150-mm square cross section. The height was 540 mm for the short specimens and 1626 mm for the longer ones.

Test variables included sustained load level, loading age, eccentricity ratio, and transverse reinforcement ratio. The concentrically loaded specimens with zero eccentricity included three plain concrete and five RC columns. Among them, one plain concrete column was tested to failure in a short time to obtain concrete compressive strength of square cross section. Two plain concrete columns were subjected to high sustained stresses to better interpret the experimental results of the RC columns and create test data for aged concrete material under sustained high stresses. For the five RC columns subjected to eccentric sustained loading, two eccentricities with respect to section centroid, e = 25.4 and 38.1 mm, were considered, corresponding to eccentricity ratios of e/h = 0.17 and 0.25, where h is column section width.

The RC column specimens were identically reinforced by four No. 3 bars with a nominal diameter of 9.53 mm. Because the actual diameter was 9 mm, D9 is used to denote these bars. The column longitudinal reinforcement ratio was 1.13%, close to the minimum column reinforcement ratio of 1% permitted by ACI 318 (ACI 2019). The thickness of concrete cover measured from the outer edge of D9 bars was 25 mm. To avoid any premature failure at column ends, each RC specimen was strengthened by four 152-mm long D16 bars bundled with the D9 bars. The transverse reinforcement consisted of 5-mm diameter (D5) hoops with seismic hooks.

ACI 318 (2019) requires the center-to-center spacing of column ties not exceed the least of 16 times the nominal diameter of longitudinal bars, 48 times the nominal diameter of tie bars, and the smallest section dimension. The first and third requirements, leading to an almost identical value of 152 mm, govern the maximum tie spacing for the RC column specimens. Two transverse reinforcement spacings, 152 and 51 mm, were considered in the tests. The corresponding transverse reinforcement ratios were $\rho_t = 0.26\%$ and 0.78%.

Table 1 shows a test matrix. The plain concrete specimen, concentrically loaded in a short time to failure, was denoted as PS. In the designations of other specimens, "P" stands for plain concrete columns loaded concentrically. "C" and "E" represent concentric and eccentric loading, respectively. The following number (e.g. 77) represents a percentage sustained load ratio α to indicate the level of sustained load. For the plain concrete columns, α is defined as the ratio of sustained load P_{sus} to the short-time axial loading capacity defined based on the test result of Specimen PS; for the RC columns under concentric loading, α is the ratio of P_{sus} to the nominal axial strength defined by ACI 318 (2019); for the RC columns under eccentric loading, α is the ratio of moment at column mid-height at the start of sustained loading to the nominal flexural strength considering axial force-moment interaction based on ACI 318 (ACI 2019). The letters A and B following the number for sustained load ratio denote specimens with a transverse reinforcement spacing of 152 and 51 mm, respectively. The last number following "A" or "B" for the eccentrically loaded RC columns indicates a percentage eccentricity ratio.

The lower level of sustained load (α = 0.76 or 0.77) was used to obtain test data for columns experiencing a relatively low rate of nonlinear concrete creep and thus having little chance of fast failure. The higher level of sustained load (α = 0.90 to 1.10) was intended to generate data for columns that may quickly fail. Therefore, α was selected as 0.90 for the concentrically loaded plain concrete column P90. For the concentrically loaded RC columns C98A and C98B, because longitudinal reinforcement can release some concrete stress during sustained loading, the sustained load level was chosen as $\alpha = 0.98$ (i.e., 98% of the code-defined nominal short-time strength). To consider a sustained load close to column actual short-time loading capacity enhanced by the confining effect of transverse reinforcement, $\alpha = 1.10$ was selected for Specimen C110A. Eccentrically loaded columns E98A17 and E99A17 were applied with sustained loads at $\alpha = 0.98$ and 0.99. Due to the higher eccentricity, E77A25 and E92A25 were expected to suffer greater 2nd order effects and thus applied with sustained loads corresponding to $\alpha = 0.91$ and 0.92.

Material Properties

Tensile tests were conducted on two samples for each size of the column reinforcement. Fig. 3a shows the stress-strain curves of a D9 and a D5 bars. The average yield stress, f_y, and elastic modulus, E_s, were 479 MPa and 208 GPa for the D9 bars. The f_y and E_s of the D5 bars were 715 MPa (0.2% offset yield stress) and 251 GPa. To minimize the unwanted influence of material property variations, all the column specimens were cast using a single batch of ready-mix concrete. Concrete cylinders, 152 mm in diameter and 305 mm in height, were companionly cast. The concrete mix per cubic meter contained 777 kg limestone, 1150 kg sand, and 307 kg Type V cement. The water-cement ratio was 0.64. Because aggregate size may affect concrete creep (Bažant and Wittmann 1983), the maximum coarse aggregate size was specified as 9.5 mm, based on the same scale factor for the column specimens. Concrete slump was 140 mm. The columns and cylinders were moisture-cured for three weeks and then demolded and stored in the air in the laboratory.

At the start as well as the completion of a sustained loading test, concrete short-time cylinder compressive strength, f_c', was determined by testing at least three samples, each loaded to failure within five minutes. Fig. 3b shows f_c' of individual cylinders at different concrete ages. No strength gain due to age was found when the concrete was beyond 200-days old; instead, f_c' was constant between ages t = 209 and 317 days and then slightly decreased by 7.9% 150 days later. Beyond t = 468 days, the average cylinder strength varied in a narrow range; thus, f_c' was again considered constant until t = 657 days when the last column test was finished. The values of f_c' defined for each specimen at the start and end of testing are given in Table 1 and shown by the dashed line in Fig. 3b. Fig. 3c shows the stress-strain curve of a concrete cylinder tested in compression at t = 546 days, where the strain was measured by strain gauges attached to the concrete cylinder at mid-height along axial direction. Concrete elastic modulus, E_c, was not measured in the cylinder tests but can be evaluated based on plane section assumption, steel Young's modulus, and the data collected during the initial short-time loading of the concentrically loaded specimens P77, P90, C76A, C98A, and C110A. The concrete secant stiffness at compressive stresses about 50% of the short-time prism strength was determined in this manner as E_c = 31.2 31.4, 29.7, 26.6, and 26.3 GPa at concrete ages of 238, 268, 317, 348, and 547 days, respectively. Because the concrete strength was stabilized after 468 days, E_c for all eccentrically loaded columns can be taken as 26.3 GPa.

Test Setup

The test setups are shown in Figs. 1 and 2. For each type of sustained loading, two sets of loading frames were prepared and seated on a steel pedestal beam anchored to a strong floor. The sustained loads were applied by tightening four 25-mm diameter high-strength posttensioning (PT) rods distributed around the four sides of a specimen at a spacing of 559 mm in one direction and 457 mm in the other. Such a loading approach is typical for testing RC or steel-concrete composite columns under sustained loads (Viest et al. 1956, Green and Breen 1969, Han et al. 2004, Jenkins and Frosch 2015, Kim et al. 2017, Cao et al. 2019). The PT force was transferred in sequence to secondary loading beams, primary loading beams, and eventually the specimen. All the loading beams were made of steel channel sections. To reduce creep-induced load drop during sustained loading, four springs were stacked in series at the upper end of each PT rod. In the columns tests by Viest et al. (1956) and Green and Breen (1969), heavy duty coil springs were used because the sustained loads were less than 260 kN. However, the highest sustained load considered in this study was almost 660 kN; accordingly, Belleville disk springs with much higher strength than coil springs were employed.

To evenly distribute the load, a 38.1-mm thick steel plate was attached to each column end by high-strength gypsum cement. For concentric loading, the specimen bore against the primary loading beam through a 25.4-mm wide, 12.7-mm thick, and 150-mm long steel strip. For eccentric loading, the load was applied to a specimen by a 25.4-mm diameter and 150-mm long steel pin located at a distance of e = 25.4 or 38.1 mm from the centerline of column section. The pin was accommodated by a 6.35-mm deep circular groove milled into the steel end plate. As shown in Fig. 2, steel channel sections were used to clamp the steel plate and column end together to ensure safety during the eccentric loading tests. The self-weight of some loading components, such as the upper loading beams and the load cells, introduced an axial force of 3.78 kN to the concentrically loaded specimens and 3.60 kN to the eccentrically loaded specimens prior to loading. These gravity forces are accounted into the total load applied to a specimen in the following discussions.

As stated previously, the collapses of several buildings under sustained loads occurred years after construction. Although concrete age at loading, t_0, is a parameter affecting concrete linear creep (ACI 209, 2008), the existing data of nonlinear creep were predominantly obtained from the tests of young concrete or RC columns ($t_0 \leq 90$ days). Accordingly, the experiments in this study were not commenced until the specimens have been constructed for more than 200 days. This loading age was also intended to reduce the increases in both concrete short-time strength and shrinkage deformation during the experimental program. Concentric load was applied to the plain concrete column PS until failure using a hydraulic jack, which was situated above the primary loading beam and bear against a steel reaction frame on the top. For the sustained concentric loading tests, initial loading was applied first by the hydraulic jack up to approximately 180 kN; the remaining load needed to reach a target sustained load was applied by the post-tensioning forces. However, for the sustained eccentric loading tests, due to the much lower needed loads, the specimens were loaded in any stage until failure purely by the tightening the PT rods. The initial loading to a target sustained load was completed typically within 90 and 60 minutes for the concentrically and eccentrically loaded specimens, respectively. To compensate load decrease due to concrete creep during sustained loading, the load was adjusted by tightening the nuts at the upper end of the PT rods while monitoring the total applied load through a data acquisition system. The load was adjusted at least daily during the first seven days when most concrete creep occurred. After that, the sustained load was maintained less frequently. If no failure occurred during sustained loading, the specimen was reloaded to failure in a short time. The hydraulic jack was used during this process for the concentrically loaded columns.

Instrumentation

The material deformations at the mid-height of a column were measured by strain gauges, as shown in Figs. 1 and 2. Concrete axial strain was measured at section mid-depth along all four column faces. To measure concrete transverse strain in the RC columns, a strain gauge was attached to a column face. For the eccentrically loaded columns, the gauge measuring concrete transverse strain was located at the compression side. Strain gauges were also mounted to two longitudinal bars near the tension face of each eccentrically loaded column. Readings from the concrete axial strain gauges were used to guide post-tensioning the rods in order to achieve a relatively even strain distribution among the four column faces during concentric loading and a symmetric strain response between the two side faces during eccentric loading. For the eccentrically loaded columns, deflections were measured at the column mid-height as well as the top and bottom ends by horizontally oriented linear variable differential transformers (LVDTs).

As shown in Figs. 1 and 2, two load cells were placed between the primary and secondary loading beams to measure the PT forces. The load applied by the hydraulic jack was measured by a load cell sitting on the primary loading beam. The laboratory is air-conditioned and located in a dry region in the U.S. with an annual precipitation of only 105 mm. Thus, the typical temperature and relative humidity inside the laboratory were 23°C and 21%, respectively.

Results of Concentric Loading Tests

Axial Stress-Strain Response and Failure Pattern

The plain concrete column PS was tested first. It was loaded to failure within 10 minutes at t_0 = 209 days. Other short columns were subjected to concentric sustained loading at t_0 between 238 and 478 days. Due to the time restraint of the experimental program, the sustained loading for Specimens C98A and C98B was terminated after 120 days when the average increase rate of axial strain during the last 5 days was less than 10^{-5}/day. For the columns subjected to lower levels of sustained load, the loading was ended much earlier when the daily strain increase has already dropped below 10^{-5} and the specimens were assumed to have little chance to fail within 120 days. Figs. 4 and 5 show the measured load-axial strain response and failure pattern of the columns. It is seen that, due to the use of disk springs, the sustained loads applied through the post-tensioning rods were relatively well maintained. Because of the square cross-sectional shape, higher slenderness, and lower loading rate, the peak stress obtained in PS was 83% of concrete cylinder strength at the same age. The result was similar to that observed in the tests by Scott et al. (1982), in which the peak stress of a plain concrete square column loaded under a comparable strain rate was 86% of cylinder strength. Based on the test result of Specimen PS, the short-time strength of a plain concrete column at zero eccentricity, is defined herein as $P_{o,c} = 0.83 f_c' A_c$, where f_c' is the short-time cylinder strength of concrete at the same age and A_c is concrete sectional area. The so-defined $P_{o,c}$ for plain concrete columns P77 and P90 at the start of sustained loading is indicated by the dashed lines in Fig. 4.

Sustained loading of Specimens P77 and P90 started from t_0 = 238 and 317 days. The average sustained load evaluated based on a 12-hours interval was P_{sus} = 425 kN = $0.77P_{o,c}$ for P77 and P_{sus} = 497 kN = $0.90P_{o,c}$ for P90. The load fluctuation due to creep and load adjustment was within 3% of P_{sus}, except for P90 during the initial 18 hours of sustained loading, when the load dropped by 8%. Because the axial strains in P77 and P90 were stabilized after 20 days, the sustained loading was terminated at $t - t_0$ = 22 days. The test result of P90 indicates that loading age plays a significant role in concrete creep and likely long-term strength under sustained high stresses. In the material tests conducted at t_0 = 28 to 56 days by Smadi et al. (1985) and Iravani and MacGregor (1998), all cylinders with a short-time strength between 21 and 69 MPa failed within 4 days if the sustained stress exceeded 80% of short-time strength; particularly, when a sustained stress of 90% of short-time strength was applied, the concrete cylinders could not endure the high stress for more than one hour and, on average, failed at an axial strain of 0.00296. In contrast, Specimen P90 (t_0 = 317 days) spent 22 days of sustained loading to reach an axial strain of 0.00196 and survived this level of high sustained stress without any sign of failure. In addition to loading age, the coarse aggregate type may also have contributed to the much lower creep rate. Under service-level sustained stresses, the creep of limestone concrete was about 60% of gravel concrete (Troxell et al. 1958). The concrete was made of limestone in this study; however, gravel was used in the tests by Iravani and MacGregor (1998). Aggregate type was not reported by Smadi et al. (1985).

After the completion of sustained loading, P77 and P90 were completely unloaded. The residual strain upon unloading was 0.00102 in P77 and 0.00118 in P90. After resting for one day, when the residual strains were reduced to 0.00096 in P77 and 0.00113 in P90, these columns were reloaded to failure within 40 minutes. During this process, the load was first increased to the previously applied sustained load by tightening the PT rods; the hydraulic jack was then used to further load the specimens to failure. As shown in Fig. 4, the unloading and reloading stiffness of P77 was similar to that during the initial loading. The peak load of P77 was P_{max} = 588 kN, exceeding $P_{o,c}$ at the end of sustained loading by 5.6%. The reloading response of P90 is not shown in Fig. 4 due to an accidental loss of strain data; however, the peak load was measured as 598 kN, 7.5% higher than $P_{o,c}$ of this specimen. Given that the cylinder compressive strength, f_c', was essentially unchanged for P77 and reduced slightly by 2.7% for P90 over the sustained loading period (Table 1), the test results of these specimens indicate that sustained loading can slightly increase concrete compressive strength. Due to the strength increase, the level of sustained stress in P90 was essentially lowered down from 90% of short-time strength at t_0 to

83% of that at the end of sustained loading, thereby significantly reducing failure likelihood. Moreover, the strength increase was accompanied with a shift from splitting failure in Specimen PS to shearing diagonal failure in P77 and P90 during reloading, as shown in Fig. 5.

For the five short RC columns, their nominal short-time axial strength at zero eccentricity, P_o, is indicated by the dashed lines in Fig. 4. P_o was evaluated based on f_c' at t_0 and ACI 318 (2019) without considering the 0.80 factor used to account for accidental eccentricity. Specimens C76A and C76B were both applied with a sustained load of P_{sus} = 518 kN = 0.76P_o at t_0 = 268 days; the load was sustained for 47 days. A high sustained load of P_{sus} = 659 kN = 0.98P_o was applied to C98A at t_0 = 348 days and C98B at t_0 = 354 days and lasted for 120 days. For these RC short columns, the largest load drop occurred only during the first day of sustained loading. The variation of sustained load from the average was less than 2.7% for each specimen.

After the completion of sustained loading, C76A, C76B, C98A, and C98B were reloaded to failure in a short time using the hydraulic jack. The reloading response is shown by the third portion of load-strain response in Fig. 4. The reloading stiffness was consistently greater than the initial loading stiffness. The peak load achieved in this loading stage was 767 kN = 1.12P_o, 797 kN = 1.16P_o, 799 kN = 1.19P_o, and 758 kN = 1.13P_o for C76A, C76B, C98A, and C98B, where P_o is defined based on f_c' measured at the end of sustained loading. As described previously, the peak load of plain concrete specimens P77 and P90 after 22-days sustained loading was 5.6% and 7.5% greater than the expected short-time strength. For the RC column specimens C76A, C76B, C98A, and C98B, the strength increase from P_o (15% on average) can be attributed to both the concrete strength gain due to sustained loading and the enhanced core concrete strength due to confinement effect. Given that the nonlinear creep of concrete is sensitive to the ratio of sustained stress to strength, the more than 10% strength increase from P_o may not be negligible when the creep of a RC column under high sustained loads needs to be accurately predicted.

Because the high sustained loads of $0.98P_o$ did not cause any failure in C98A and C98B and their reloading strength was 16% higher than P_o, the sustained load applied to Specimen C110A was increased to 699 kN = $1.10P_o$ so that it could fail quickly during sustained loading. The initial loading resulted in a concrete axial strain of 0.00200. After only 2.55 minutes of sustained loading, the specimen suddenly failed at an axial strain of 0.00225 when the load dropped by 1.3% to 690 kN.

Load Redistribution in RC Columns during Sustained Loading

Assuming that concrete was linear elastic prior to reaching a load of 130 kN, concrete Young's modulus was estimated for each RC column based on the plane section assumption, measured concrete axial strain, and steel elastic modulus. The free shrinkage strain of concrete material was not measured in the tests but estimated according to the formulations recommended by ACI 209 (ACI 2008), concrete age, environment temperature, and relative humidity. Based on concrete free shrinkage, the initial stresses and strains in concrete and steel due to restrained concrete shrinkage prior to loading were predicted based on deformation compatibility and equilibrium. The net axial force carried by the four D9 longitudinal bars, N_s, during the initial and sustained loading was determined according to their initial stress caused by concrete shrinkage, the measured concrete axial strain, and the material property of the D9 bars. The net axial force resisted by concrete, N_c, was then evaluated by deducting N_s from the measured load.

The variations of N_s and N_c during sustained loading are shown in Fig. 6 for Specimens C76A, C76B, C98A, and C98B. Time is indicated using logarithmic scale in the figure. N_c decreased with time; however, the reduction was limited because the axial force in a column was primarily carried by concrete due to the relatively low longitudinal reinforcement ratio. The total yield force of the four column longitudinal bars was 122 kN. These bars reached yielding in Specimen C76B at $t - t_0 = 3$ days. No yielding was predicted for C76A during the 47-days sustained loading. Steel yielding occurred in C98A and C98B soon after the start of sustained loading at $t - t_0 = 5$ and 7 hours. After steel yielding, the average stress sustained in concrete was 24.1 MPa, a value exactly equal to the short-time concrete strength for square section ($0.83f_c'$) at t_0. Apparently, the transverse reinforcement must have enhanced the strength of core concrete so that C98A and C98B could carry the sustained loads for 120 days without any failure.

Creep Development

Table 2 summaries the key concrete deformation properties during the sustained concentric loading of the RC short columns. Compared with the large instantaneous and creep strains caused by the high loads, shrinkage strain should be very limited. For each specimen, the estimated concrete tensile strain due to restrained shrinkage prior to loading was less than 6% of the axial compressive strain caused by initial loading; moreover, because $t_0 > 230$ days, the change in predicted concrete free shrinkage strain over the sustained loading period accounted for at most 3% of the measured creep strains. Thus, the effects of shrinkage during sustained loading are neglected and a creep coefficient, φ, is defined based on the axial strains at the start and end of sustained loading given in Table 2.

Fig. 7 plots the development of creep during sustained loading. As shown in Fig. 7a, in the first day of sustained loading, axial strain rapidly increased by 36% in P77, 30% in P90, 25% in C76A, 26% in C76B, 36% in C98A, and 17% in C98B. The creep rate then decreased with time. Even if the sustained load ratio of P90 ($t_0 = 317$ days) was 17% greater than that of P77 ($t_0 = 238$ days), φ was slightly lower in P90 until $t - t_0 = 7.4$ days and became nearly identical thereafter. Apparently, the 79-days difference in loading age affected φ. After 20 days of loading, the axial strain in both columns became stabilized and, when the sustained loading was stopped at $t - t_0 = 22$ days, φ was equal to 1.00 for P77 and 0.99 for P90.

Specimens C76A with $\rho_t = 0.26\%$ and C76B with $\rho_t = 0.78\%$, subjected to a sustained load of $0.76P_o$, presented nearly same creep response, as indicated in Fig. 7b. At $t - t_0 = 47$ days when the sustained loading was stopped, φ was equal to 0.86 for both columns. Thus, the difference in transverse reinforcement ratio did not cause any impact on creep coefficient of these columns. However, the effects of column transverse reinforcement on creep became notable when a high sustained load of $0.98P_o$ was applied. As shown in Fig. 7c, the φ of C98B was 77%, 51%, and 28% less than that of C98A at $t - t_0 = 1$ hour, 1 day, and 7 days, respectively. Because the sustained loading of C98B started only 6 days later than C98A, the difference in φ should not be attributed to loading age. However, the creep discrepancy decreased with time and, when the sustained loading was ended at $t - t_0 = 120$ days, φ = 1.14 for C98A and 1.13 for C98B.

Comparison of creep coefficient is also made between C98A and the plain concrete column P90 to examine the effects of transverse reinforcement. By $t - t_0 = 22$ days (when the sustained loading of P90 was ended), φ of C98A was 0.708, nearly 30% lower than that of P90. Even if the t_0 of C98A was 31 days greater, both specimens were loaded at an age beyond 310 days and therefore loading age effect should be less pronounced. Moreover, the level of concrete sustained stress in C98A was 11% greater than in P90. Thus, the difference in creep deformation between the two specimens should be attributed mainly to the confinement effect of transverse reinforcement in C98A. It follows that, even with the largest spacing permitted by design code, the ties having seismic hooks can protect a RC column again failure under high sustained concentric loads.

Transverse Deformation

The transverse strains of concrete cover measured at column mid-height, ε_{ct}, during sustained loading are shown in Fig. 8 and Table 2 for the concentrically loaded RC columns. The transverse strain ε_{ct} at the beginning of sustained loading was consistently greater for the columns subjected to higher loads. During sustained loading, ε_{ct} changed little in Specimen C76B and even decreased in C76A. This explains that, in spite of the different transverse reinforcement ratios, the two specimens presented almost identical creep response. In contrast, in C98A and C98B, the two columns subjected to higher sustained loads, the transverse deformation was more than tripled over time. The trend of reduced difference in ε_{ct} between these specimens was consistent with that of the creep response shown in Fig. 7c. It is likely that, due to the higher ρ_t, the core concrete of C98B attracted greater stress than C98A and was thus softened quicker as time elapsed. This caused a portion of the stress initially carried by the core to be redistributed to the cover so that the difference in both creep coefficient (Fig. 7) and transverse strain (Fig. 8) between C98A and C98B was reduced toward the end of sustained loading. Because Specimen C110A failed soon after the start of sustained loading, transverse strain increased by only 10%. The distinctively different transverse strain responses under two levels of sustained load (α = 0.76 and α = 0.98) affected the transverse strain during the subsequent reloading to failure. The ε_{ct} measured at the peak load reached 0.00227 and 0.00233 in C98A and C98B but was only 0.000216 and 0.000753 in C76A and C76B.

Based on the measured axial and transverse strains, the Poisson's ratio of concrete cover, v, was computed for each RC column during sustained loading and shown in Fig. 9 and Table 2. The evolution trend of v was similar to that of concrete transverse strain. For both C76A and C76B, v was equal to 0.23 at t_0 and decreased during sustained loading. For C98A and C98B, v

was equal to 0.29 and 0.21 at t_0. The lower v in C98B was most likely caused by greater confinement effect. After one day of sustained loading, v quickly increased by 0.08 in C98A and 0.06 in C98B. The difference in v between C98A and 98B decreased over time; by the end of sustained loading for 120 days, v was equal to 0.45 in C98A and 0.42 in C98B. The Poisson's ratio of C110A was 0.35 at the start of sustained loading and quickly increased to 0.41 at failure. The variation trend of v was consistent with the findings made from the tests of young concrete material (Stöckl 1972; Mazzotti and Savoia 2002). Firstly, ν increased over time when the sustained stress was greater than 80% of concrete short-time strength but remained unchanged or even decreased when the sustained load was moderate. Secondly, v at failure increased for concrete under reduced level of sustained stress; accordingly, even if the v of C98A and C98B exceeded that of C110A, no failure occurred.

Results of Eccentric Loading Tests

Load – Moment Response and Failure Pattern

The sustained eccentric loading tests of RC columns were conducted between t_0 = 547 and 629 days, when concrete strength can be taken as constant, as indicated in Fig. 3b. The overall performance is shown in Fig. 10 by the axial force versus mid-height moment response. Second order effects were not obvious during the initial loading when the load was lower than 100 kN. Also shown in Fig. 10 is a sectional interaction diagram defined based on ACI 318 (2019) to indicate the nominal short-time flexural strength of columns, M_n, at different axial forces. Only one column, E99A17, failed during sustained loading. All other columns underwent three loading stages: initial loading, sustained loading, and reloading to failure. Similar to the concentric loading tests, the largest load drop occurred during the first day of loading but was lower than 2.5% of the target sustained load; in the remaining period of sustained loading, the loads were maintained with less fluctuation. The sustained loading was terminated when the average deflection increase rate at column mid-height was at most 0.05 mm/day.

The initial loads applied to the columns with an eccentricity ratio of e/h = 0.17 were chosen to generate a mid-height moment, M, close to the code-defined nominal flexural strength at a particular axial force, M_n. Accordingly, a sustained load of P_{sus} of 387 kN ($0.60P_o$), 362 kN ($0.57P_o$), 382 kN ($0.60P_o$) was applied to Specimens E98A17, E99A17, and E100B17, leading to an initial center deflection of Δ = 5.03, 8.71, and 6.40 mm and $M = 0.98M_n$, $0.99M_n$, and M_n, respectively. From $t - t_0$ = 18 days for E98A17 and 6 days for E100B17, the daily deflection increase became less than 0.05 mm. When the sustained loading was terminated at $t - t_0$ = 22 days for E98A17 and 11 days for E100B17, deflection Δ reached 10.8 and 9.94 mm, causing an 18.7% and 11.1% increase in mid-height moment, respectively. The peak load during reloading was achieved at Δ = 11.5 mm in E98A17 and 10.5 mm in E100B17. The moment at the peak axial load, M_{max}, was $1.33M_n$ for E98A17 and $1.28M_n$ for E100B17. As described previously for the concentrically loaded column C110A, confinement effect enhanced its short-time strength by approximately 10%; this effect, however, should be less pronounced in the flexural strength of an eccentrically loaded column. Accordingly, the extra strength of E98A17 and E100B17 beyond M_n may be partially attributed to the strength increase due to the previously applied sustained loads. Specimen E99A17 endured the sustained load for only 53 hours and failed at Δ = 13.2 mm when a load adjustment was made. The failure moment was 12% greater than M_n. The strength gain of this specimen from sustained loading was limited due to the short loading period; as a result, the extent of strength increase from M_n was the lowest among the three columns with an eccentricity ratio of 0.17.

Specimen E77A25 with e/h = 0.25 was initially applied with a load of P_{sus} = 247 kN (0.39P_o), resulting in a deflection of Δ = 5.49 mm and a mid-height moment of M = 0.77M_n. The load was sustained for 11 days, over which Δ was increased by only 1.19 mm and M by 5.5%. The load was then increased to 274 kN (0.43P_o), causing Δ = 7.20 mm and M = 0.91M_n. During the second sustained loading of 17 days, Δ was increased by 1.07 mm, leading to only a 2.5% moment increase. The low increase in deflection in both loading stages made the sustained loading effect almost indiscernible in Fig. 10d. When reloaded, E77A25 failed at Δ = 13.3 mm with M_{max} = 1.34M_n. Specimen E92A25 was initially loaded to P_{sus} = 270 kN (0.42P_o), causing Δ = 8.19 mm and M = 0.92M_n. After 28 days of sustained loading, Δ increased to 12.8 mm, resulting in an 11% moment increase. During the subsequent reloading, peak load occurred at Δ = 13.4 mm and the corresponding moment M_{max} was 12% greater than M_n.

For the design of non-sway columns, ACI 318 (2019) employs a moment amplification factor, δ, to increase first-order moment, thereby accounting for the effects of second-order deformation and creep. Neglecting the strength and stiffness reduction factors associated with reliability, δ is expressed as

$$\delta = \frac{1}{1 - \frac{P_{sus}}{P_c}} \qquad \text{Eq. (1)}$$

where P_c is critical buckling load and defined by Eq. (2) for single curvature columns.

$$P_c = \frac{\pi^2 E_c I}{(1 + \beta_{dns}) l_u^2} \qquad \text{Eq. (2)}$$

where β_{dns} is a parameter accounting for stiffness reduction due to creep effect, E_cI is section flexural rigidity during short-time loading, and l_u is unsupported length of column. Based on its definition, β_{dns} = 0 if only short-time loading is considered, and β_{dns} = 1 if only sustained load exists after the initial short-time loading (i.e., no other type of load participates in loading combination).

The effectiveness of Eqs. (1) and (2) was examined by the results of the five eccentrically loaded columns tested in this study. The curvature measured at column mid-height at the end of initial short-time loading (described later in this paper) was used to define E_cI in Eq. (2). The center distance between the two pins at column ends was used to define l_u. E99A17 failed during sustained loading; thus, the moment amplification factor was examined only for short-time loading for this column. E77A25 experienced two levels of sustained loading; thus, test data for the first level were considered. Fig. 11 compares the predicted and measured results. On average, the ACI 318 approach underestimates 13% of the bending moment amplified by 2nd order effect during the initial short-time loading. However, due to the crude nature of parameter β_{dns}, there is a notable difference between the predicted and measured values for the extra bending moment caused by sustained loading. Particularly, compared with the experimental result, the ACI 318 approach more than triples the moment increase in the sustained loading stage for E100B17 and E77A25. Based on the observed creep rate at the end of sustained loading, the large discrepancy would not be dramatically reduced even if these specimens can be loaded for a longer time.

Fig. 12 shows the crack pattern and failure mode of the eccentrically loaded columns. Flexural cracks were not visible during the initial loading and the first day of sustained loading of the columns with e/h = 0.17. For the columns with e/h = 0.25, cracks were noticed in the column mid-height region immediately after the initial loading. The failure of Specimens E98A17, E99A17, E77A25, and E92A25 was brittle and accompanied with severe buckling of the column longitudinal bars at mid-height. However, rebar buckling did not occur at the failure of E100B17 where the transverse reinforcement spacing was reduced.

Axial Strains

The measured axial strains indicate that plane section assumption was approximately held during both short-time and sustained loading. Moreover, along the loading path, the pin at each beam end caused a distributed bearing stress on the steel plate due to contact. The resultant force of the bearing stress ideally should be aligned with pin center; otherwise, the actual eccentricity would deviate from the nominal value. The strain measurements were used to partially validate the eccentricity ratios defined for the specimens. Fig. 13 shows column mid-height axial strains measured in Specimens E100B17 and E92A25 at four locations, including tension face, tensile reinforcement, mid-depth of side faces, and compression face. When the load was low so that the second order effect was negligible and the columns behaved elastically, the axial strain should be approximately equal to zero at the tension face of the columns with e/h = 0.17 and in the tensile reinforcement of the columns with e/h = 0.25. As shown in Fig. 13, such a strain condition was achieved when axial load was below 100 kN.

The axial strain at compression face, ε_c, could not be captured in Specimen E98A17 due to strain gauge malfunction. For Specimens E99A17, E100B17, E92A25, and E77A25, the initial loading caused ε_c = 0.00273, 0.00264, 0.00208, and 0.00164. Thus, the compressive stress at concrete cover of the first three specimens should already be in the descending branch of stress-strain response. By the end of sustained loading, ε_c was increased to 0.00368 in E100B17 and 0.00329 in E92A25. The ultimate compressive strain, ε_{cu}, at the failure of E99A17 during sustained loading was 0.00417. The ε_{cu} for other specimens, which survived the sustained loading and were reloaded to failure, was similar to that of E99A17 and equal to 0.00482, 0.00394, and 0.00454 for E100B17, E92A25, and E77A25, respectively. As expected, and shown in Fig. 13, when the peak load was reached, the tensile reinforcement has not yielded so that the failure of each specimen was governed by concrete crushing. Viest et al. (1956) stated that the ultimate strain of concrete following sustained loading may be approximated by superimposing the concrete ultimate strain under short-time loading with creep strain. This observation, however, was made from the tests of 13 columns with only one loaded at an age greater than 90 days, and is thus examined herein. After subtracting the creep strains, ε_{cu} becomes 0.00378, 0.00273, and 0.00376 for Specimen E100B17, E92A25, and E77A25, with an average of 0.00342, sufficiently close to the typical concrete ultimate strains under short-time loading.

Moment-Curvature Response

Based on plane section assumption, the axial strains measured at the column side and compression faces were used to calculate column mid-height curvature, from which a moment-curvature response was constructed and shown in Fig. 14. Because the axial strain at compression face was unavailable for Specimen E98A17, its curvature was determined from the axial strains measured at the tensile reinforcement and the side faces. E98A17 had the highest flexural stiffness during initial loading, whereas the stiffness of remaining columns was similar. Compared with the initial loading, concrete creep caused by sustained loading significantly softened the columns; however, the stiffness during this loading stage was approximately constant. Based on the moments and curvatures at the start and end of sustained loading, a secant flexural stiffness was calculated. This stiffness during sustained loading was nearly identical in E98A17 and E99A17; in comparison, the stiffness of E100B17 with reduced transverse reinforcement spacing was 21% higher, which contributed to the lower creep effects discussed later. The ultimate curvatures at failure were comparable among E98A17, E99A17, E100B17, and E92A25. Specimen E77A25 achieved higher flexural strength and deformation capacity than E92A25, which may be explained by the different sustained loading histories.

Creep for Deflection and Curvature

Two types of creep were examined: column center deflection representing global deformation and mid-height curvature reflecting local deformation. Such deformation properties measured at the start and end of sustained loading are summarized in Table 3. The variation of creep coefficient, φ, over time during sustained loading is shown in Figs. 15 and 16. Load was initially applied to E98A17, E99A17, and E100B17 at t_0 = 547, 604, and 603 days, respectively. Even if E98A17 was loaded 57 days earlier than E99A17, they had similar φ during the first two days of sustained loading, as shown in Fig. 15. This indicates that the difference in loading age was not influential for the eccentrically loaded columns, which were already more than 500-days old at the start of testing. E100B17 had the lowest φ among the three specimens with e/h = 0.17 and remained intact during sustained loading; however, E99A17 quickly failed within three days of loading. On the other hand, after 10 days of sustained loading, the φ for E100B17 was 45% lower for deflection and 67% lower for curvature than those for E98A17. Thus, the test data of E98A17, E99A17, and E100B17 revealed that increasing transverse reinforcement ratio can reduce creep deformations in an eccentrically loaded column carrying high sustained loads.

The creep coefficients for E77A25 during the first and second sustained loading, which started at t_0 = 629 and 640 days, are shown separately in Fig. 16. Due to the lower load, φ during the first sustained loading of 11 days was less than 50% of that for Specimen E92A25 loaded at nearly the same age. Even if the second sustained load applied to E77A25 resulted in an initial mid-height moment comparable to that of E92A25, the φ in term of either deflection or curvature of E77A25 was lower than in its first sustained loading and much less than that of E92A25. Thus, the test of E77A25 indicated a history-dependent creep behavior of RC columns: the lower sustained load applied previously reduced the creep deformation caused by the higher sustained load applied later.

The creep deformation of E92A25 is compared with that of a column tested by Jenkins and Frosch (2015). This column, designated as R3-40-25-LT(1), had the same column section size, eccentricity ratio, and longitudinal reinforcement ratio; other properties, including column slenderness and transverse reinforcement ratio, were similar. Compared to E92A25, R3-40-25-LT(1) was applied with a lower level of sustained load ($P_{sus} = 0.35P_o$), thereby causing an 38% lower initial deflection. However, the deflection after 28 days of sustained loading was 48% higher than E92A25 and the corresponding creep coefficient φ was as high as 2.75, far exceeding φ = 0.562 in E92A25. The use of gravel as coarse aggregate in R3-40-25-LT(1) can partially explain its high value of φ. However, the early loading age of t_0 = 53 days for R3-40-25-LT(1) may have dominated the considerably different creep response. This indicates that, if a greater accuracy is desired, column design approach should incorporate the effects of aggregate type and loading age.

Transverse Deformation at Compression Face

The variations of concrete transverse strain, ε_{ct}, and Poisson's ratio, ν, at the compression face of column mid-height during sustained loading are shown in Figs. 17 and 18 for four columns. Higher level of load caused greater transverse strain. After initial loading, ε_{ct} = 0.00137, 0.00117, and 0.00081, and ν = 0.50, 0.45, and 0.39 in Specimens E99A17, E100B17, and E92A25, respectively. Similar to the concentric loading tests, the evolution of Poisson's ratio during sustained loading was impacted mainly by transverse strain. After loading for one day, ν increased to 0.48 and 0.42 in E100B17 and E92A25; after three days, ν became stabilized at around 0.50 in E100B17, whereas ν in E92A25 varied in a narrow range of 0.40 to 0.44. In contrast, ε_{ct} and ν quickly increased to 0.00259 and 0.69 in E99A17 by the end of the first day's loading and kept increasing thereafter. When this specimen failed during the third day of sustained loading, ε_{ct} was equal to 0.00359 and ν reached 0.86. For Specimen E77A25, ν was 0.19 after the initial loading and slightly reduced to 0.15 after 11 days; even if the sustained load was then increased, ν showed little change and was equal to 0.17 by the end of the second sustained loading. When E100B17, E92A25, and E77A25 failed during reloading, ε_{ct} = 0.00283, 0.00202, and 0.00208, and ν = 0.59, 0.51, and 0.46, respectively.

Conclusions

Sustained concentric and eccentric loading tests were conducted on plain concrete and reinforced concrete columns at ages greater than 200 days. The levels of sustained load ranged from 76% to 110% of the predicted column nominal short-time strength. The following major observations and conclusions were reached:

- The creep of concrete under sustained high stresses was affected by loading age and coarse aggregate type. The aged concrete columns constructed with limestone aggregates demonstrated high strength to carry heavy sustained loads. The concentrically loaded columns resisted a sustained load as high as 98% of column short-time strength for 120 days. Moreover, no column failed during eccentric loading if the initial moment caused by sustained loads was no more than 92% of short-time flexural strength.
- Under a high sustained load close to a column's short-time capacity, the confinement effects provided by transverse reinforcement resulted in lower creep deformation, thereby reducing the risk of column failure under sustained loading. Under concentric loading, the beneficial effect of higher transverse reinforcement ratio was prominent during the

early sustained loading stage but diminished over time. More experiments are needed to further examine the effects of transverse reinforcement on concrete creep.

- Previous sustained loading increased the residual short-time loading capacity of columns. On average, sustained loading increased the short-time strength of plain concrete columns by 6.6%. The combined effects of sustained loading and transverse reinforcement confinement increased the axial strength of reinforced concrete columns by 12% to 19% and flexural strength by 11% to 33%.
- The Poisson's ratio of concrete cover can be taken as an indicator of column safety under sustained loading. No failure occurred during either concentric or eccentric loading, if the Poisson's ratio of concrete cover increased only slightly or decreased. In contrast, two columns that failed during sustained concentric and eccentric loading experienced a fast increase in Poisson's ratio when the failures were approached.
- Due to concrete creep, the flexural stiffness at the column critical section during sustained eccentric loading was much lower than that prior to the application of sustained loading. The flexural stiffness during sustained loading was approximately constant and about 20% higher when column transverse reinforcement ratio was tripled.
- The test of an eccentrically loaded column experiencing two levels of sustained load indicated that the lower sustained load applied earlier reduced creep effects under the higher sustained load applied later. In spite of the different loading histories, the compressive strain of concrete at failure after deducting creep-induced strain was similar to the ultimate strain of concrete under short-time loading.

- The ACI 318 moment amplifier approach for eccentrically loaded columns is too rough to accurately estimate the extra bending moment caused by creep deformation during sustained loading.

Acknowledgements

This paper is based on work supported by the National Science Foundation (NSF) under Grant No. 1762362 and 1760915. The authors gratefully acknowledge the financial support from NSF. The opinions, findings, and conclusions or recommendations expressed in this paper are those of the authors and do not necessarily reflect the views of the sponsor.

Data Availability Statement

Experimental data that support the findings of this study are available from the corresponding author upon reasonable request.

References

ACI (American Concrete Institute). 2019. *Building code requirements for structural concrete and Commentary*. ACI 318. Farmington Hills, MI: ACI.

ACI (American Concrete Institute). 2008. *Guide for Modeling and Calculating Shrinkage and Creep in Hardened Concrete*. ACI 209. Farmington Hills, MI: ACI.

Awad, M.E. and Hilsdorf, H.K. (1971). "Strength and Deformation Characteristics of Plain Concrete Subjected to High Repeated and Sustained Loads," Structural Research Series No. 372, University of Illinois.

Bažant, Z. P. and Wittmann F. H. (1983). *Creep and Shrinkage in Concrete Structures*, John Wiley & Sons, 374 pp.

Cao, G., Han, C., Peng, P., Zhang, W., and Tang., H. (2019). "Creep Test and Analysis of Concrete Columns under Corrosion and Load Coupling." *ACI Structural Journal*, 116(6), 121-130.

Green, R. and Breen, J.E. (1969). "Eccentrically Loaded Concrete Columns under Sustained Load," *ACI Journal*, 66(11), 866-874.

Green, R. and Breen, J. E. (1984). "Eccentrically Loaded Concrete Columns: 15 Years of Sustained Load," IABSE congress report, 911-918.

Goyal, B.B. and Jackson, N. (1971). "Slender Concrete Columns under Sustained Load," *Journal of the Structural Division*, 97(11), 2729-2750.

Guimarães, G.B. and Silva, R.R. (2001). "Analysis of the Structural Collapse of a 26-Story Building," *Rehabilitating and Repairing the Buildings and Bridges of the Americas Conference*, 186-201.

Han, L., Tao, Z., and Liu, W. (2004). "Effects of Sustained Load on Concrete-Filled Hollow Structural Steel Columns." *Journal of Structural Engineering*, 130(9), 1392-1404.

Iravani, S. and MacGregor, J.G. (1998). "Sustained Load Strength and Short-Term Strain Behavior of High-Strength Concrete," *ACI Structural Journal*, 95(5), 636-647.

Jenkins, R.W. and Frosch, R.J. (2015). "Improved Procedures for the Design of Slender Structural Concrete Columns," Concrete Research Council, American Concrete Institute.

Khalil, N., Cusens, A.R., and Parker, M.D. (2001). "Tests on Slender Reinforced Concrete Columns," *Structural Engineer*, 79(18), 21-30.

Kim, C.-S., Park, H.-G., Choi, I.-R., and Chung, K.-S. (2017). "Effect of Sustained Load on Ultimate Strength of High-Strength Composite Columns Using 800-MPa Steel and 100-MPa Concrete." *Journal of Structural Engineering*, 143(3), 04016189.

Mazzotti, C. and Savoia, M. (2002). "Nonlinear Creep, Poisson's Ratio, and Creep-Damage Interaction of Concrete in Compression, *ACI Material Journal*, 99(5), 450-457.

Mazzotti, C. and Savoia, M. (2003). "Nonlinear Creep Damage Model for Concrete under Uniaxial Compression," *Journal of Engineering Mechanics*, 129(9), 1065-1075.

Rüsch, H. (1960). "Researches toward a General Flexural Theory for Structural Concrete," *ACI Journal Proceedings*, 57(7), 1-28.

Shah, S.P. and Chandra, S. (1970). "Fracture of concrete subjected to cyclic and sustained loading," *ACI Journal Proceedings*, 67(10), 739-758.

Smadi, M.M., Slate, F.O., and Nilson, A.H. (1985). "High, Medium, and Low-Strength Concretes Subject to Sustained Overloads - Strains, Strengths, and Failure Mechanisms," *ACI Journal*, 82(5), 657-664.

Stöckl, S. (1972). "Strength of Concrete under Uniaxial Sustained Loading," ACI Special Publication, SP34-16, 313-326.

Tasevski, D., Ruiz, M.F., and Muttoni, A. (2018). "Compressive Strength and Deformation Capacity of Concrete under Sustained Loading and Low Stress Rates," Journal of Advanced Concrete Technology, 16(8), 396-415.

Thean, L.P., Vijiaratnam, A., Lee, S.-L., and Broms, B.B. (1987). Report of the Inquiry into the Collapse of Hotel New World. Singapore: Singapore National Printers.

Troxell, G. E., Raphael, J. M. and Davis, R. E., (1958). "Long-Time Creep and Shrinkage Tests of Plain and Reinforced Concrete," *ASTM Proceedings*, 58, 1101-1120.

Viest, I.M., Elstner, R.C., and Hognestad, E. (1956). "Sustained Load Strength of Eccentrically Loaded Short Reinforced Concrete Columns," *ACI Journal Proceedings*, 52(3), 727-754.

Table 1. Test Matrix

Specimen	Loading type	Sustained load ratio α	Transverse reinf. ratio (%)	Eccentricity ratio	Loading age t_0 (days)	Duration of sustained load t_d (days)	Concrete strength f_c' (MPa)	
							t_0	$t_0 + t_d$
PS	Concentric	–	–	0	209	–	29.8	–
P77	Concentric	0.77	–	0	238	22	29.8	29.8
P90	Concentric	0.90	–	0	317	22	29.8	29.0
C76A	Concentric	0.76	0.26	0	268	47	29.8	29.8
C76B	Concentric	0.76	0.78	0	268	47	29.8	29.8
C98A	Concentric	0.98	0.26	0	348	120	29.0	27.4
C98B	Concentric	0.98	0.78	0	354	120	29.0	27.4
C110A	Concentric	1.10	0.26	0	478	0.0018*	27.4	27.4
E98A17	Eccentric	0.98	0.26	0.17	547	22	27.4	27.4
E99A17	Eccentric	0.99	0.26	0.17	604	2.237*	27.4	27.4
E100B17	Eccentric	1.00	0.78	0.17	603	11	27.4	27.4
E77A25	Eccentric	0.77/0.91	0.26	0.25	628	11/17	27.4	27.4
E92A25	Eccentric	0.92	0.26	0.25	629	28	27.4	27.4

* failed during sustained loading.

Table 2. Deformations of concrete during sustained eccentric loading

Specimen	Duration (days)	Axial strain (10^{-3})		Creep coefficient	Transverse strain (10^{-3})		Poisson's ratio	
		beginning	end		beginning	end	beginning	end
P77	22	0.857	1.70	0.99	–	–	–	–
P90	22	0.984	1.96	1.00	–	–	–	–
C76A	47	0.742	1.38	0.86	0.170	0.111	0.229	0.081
C76B	47	1.22	2.27	0.86	0.277	0.326	0.227	0.142
C98A	120	1.30	2.77	1.14	0.531	1.638	0.287	0.454
C98B	120	1.48	3.15	1.13	0.432	1.821	0.214	0.415
C110A*	0.0018	2.00	2.25	0.12	0.700	0.919	0.350	0.409

* failed during sustained loading

Table 3. Deflection and Curvature during Sustained Eccentric Loading

Specimen	Duration (days)	Deflection			Curvature		
		beginning (mm)	end (mm)	creep coefficient	beginning (10^{-3}/m)	end (10^{-3}/m)	creep coefficient
E98A17	22	5.03	10.8	1.15	11.9	31.4	1.64
E99A17	2.237*	8.72	13.3	0.516	24.4	38.9	0.594
E100B17	11	6.40	9.94	0.553	22.3	32.2	0.442
E77A25 (1st)	11	5.49	6.68	0.217	18.3	22.1	0.207
E77A25 (2nd)	17	7.19	8.27	0.149	23.8	26.9	0.124
E92A25	28	8.19	12.8	0.562	21.5	35.1	0.632

* failed during sustained loading

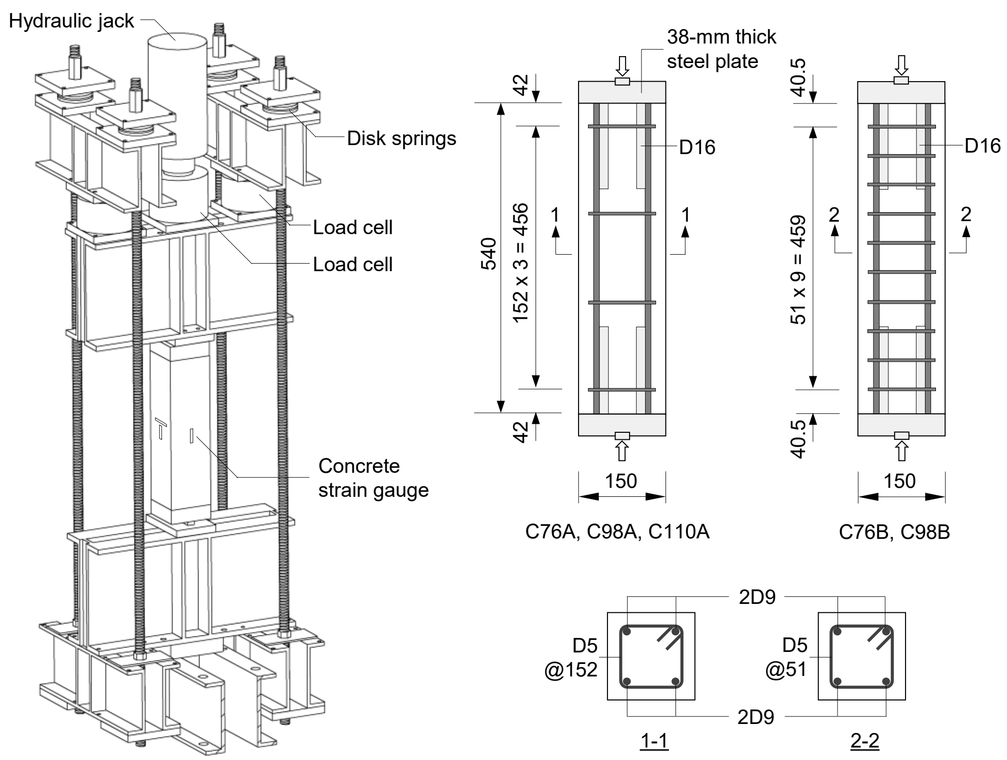

Fig. 1. Test setup and reinforcing detail for concentrically loaded columns (dimension in mm).

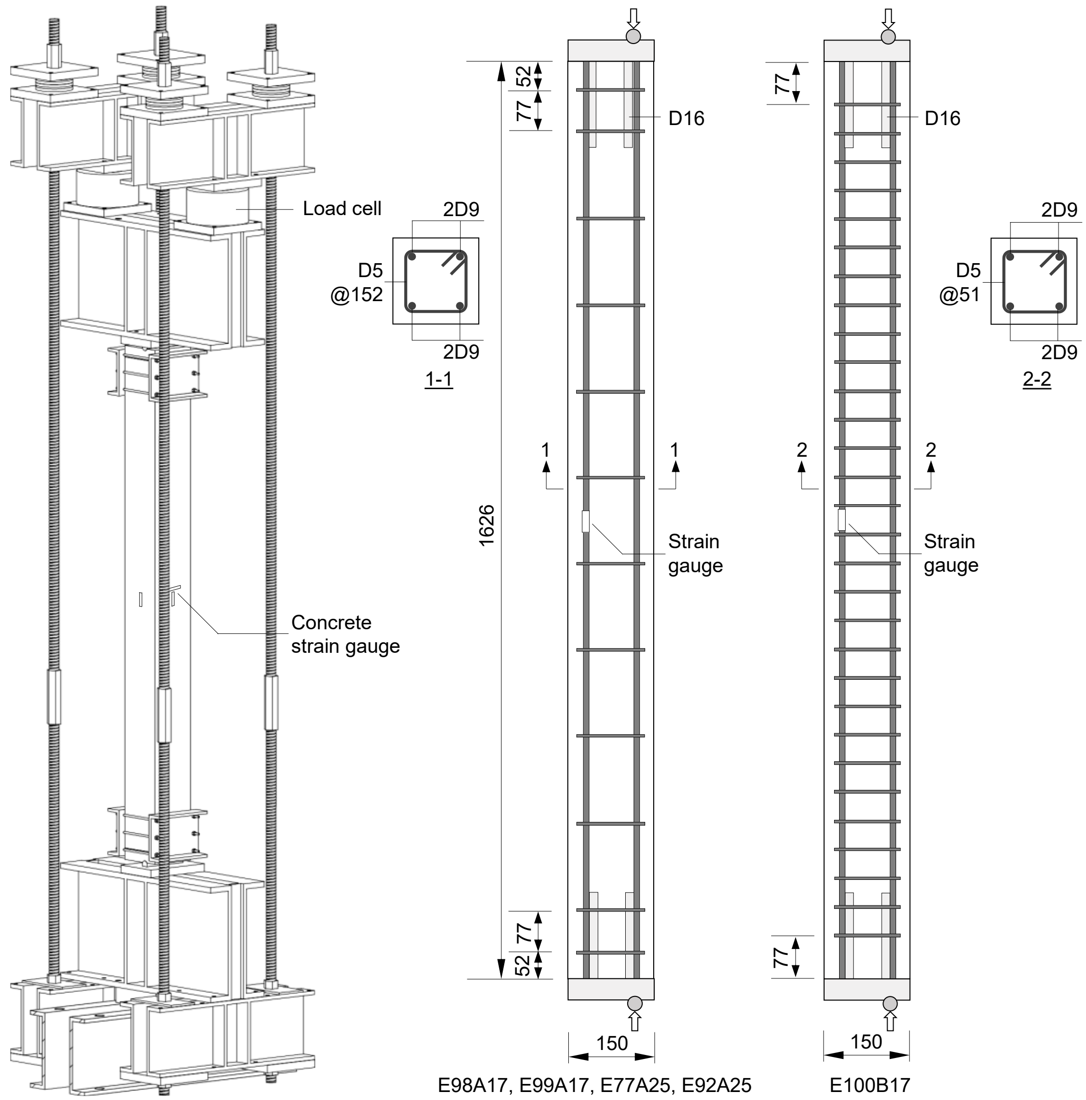

Fig. 2. Test setup and reinforcing details for eccentrically loading columns (dimension in mm).

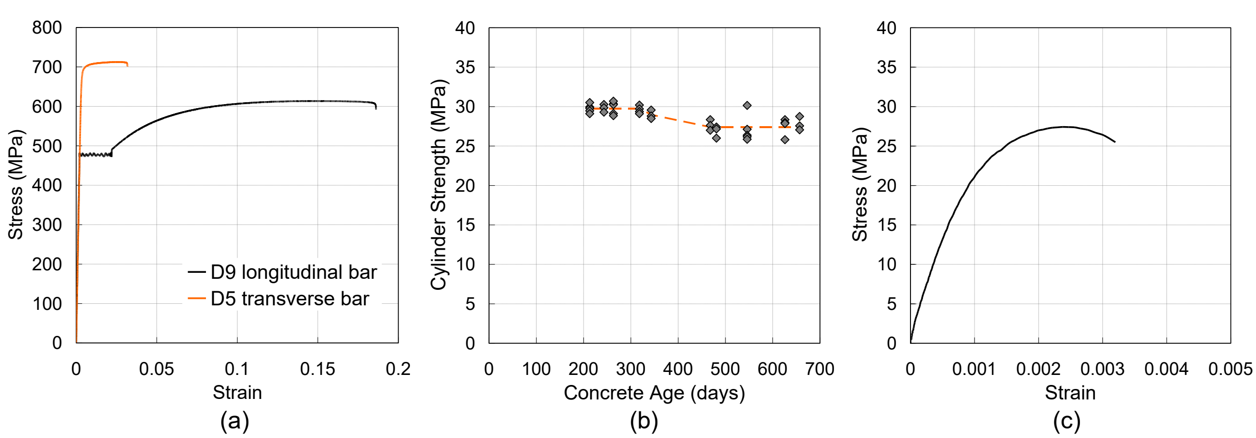

Fig. 3. Material properties: (a) reinforcement stress-strain response, (b) concrete cylinder compressive strength over time, and (c) a sample stress-strain response of concrete cylinder in short-time loading.

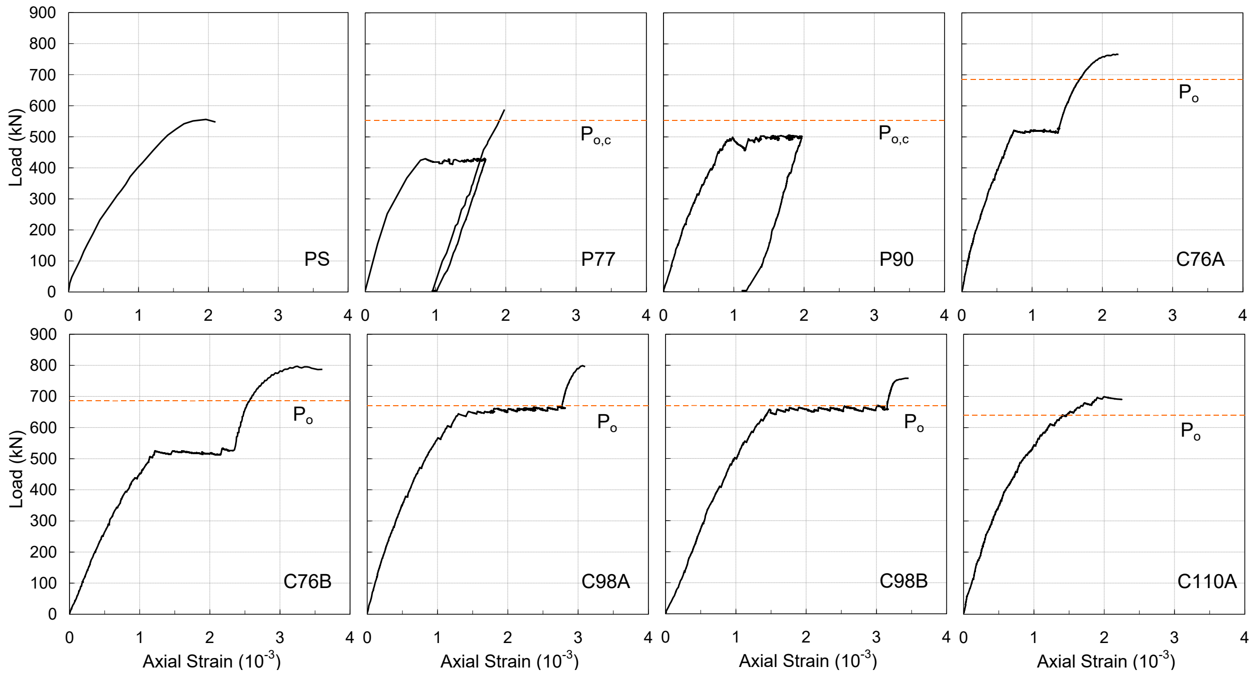

Fig. 4. Load-axial strain response of concentrically loaded columns.

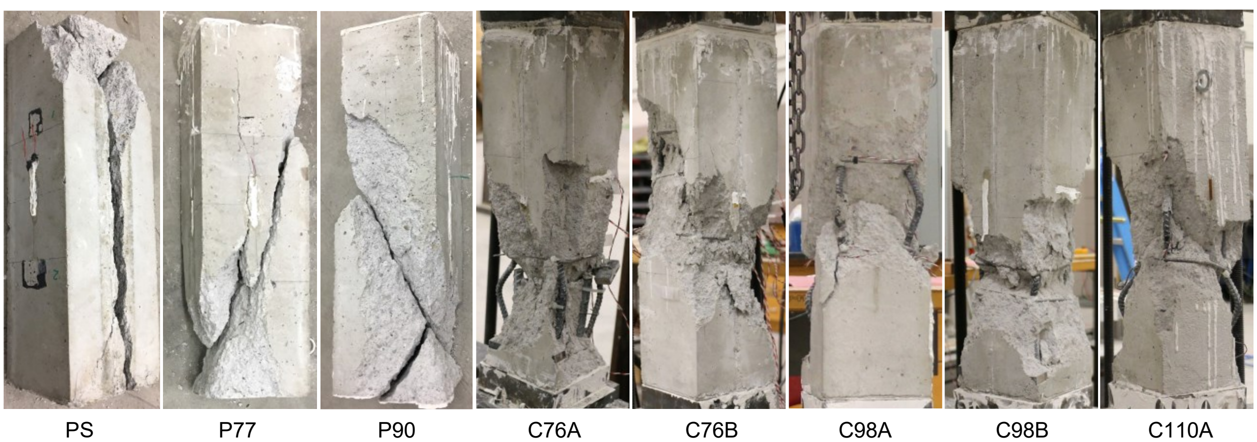

Fig. 5. Failed columns after concentric loading.

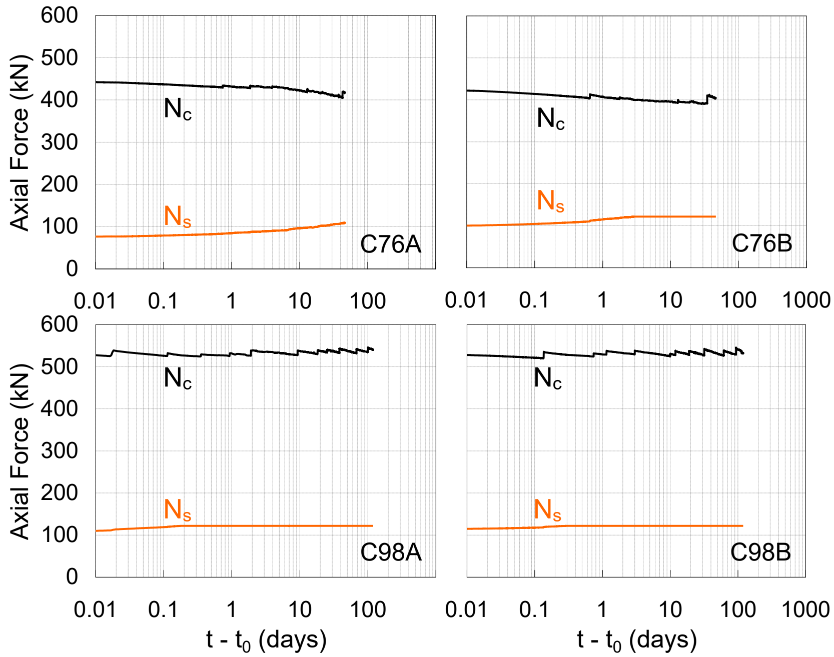

Fig. 6. Axial forces resisted by concrete and steel during sustained concentric loading.

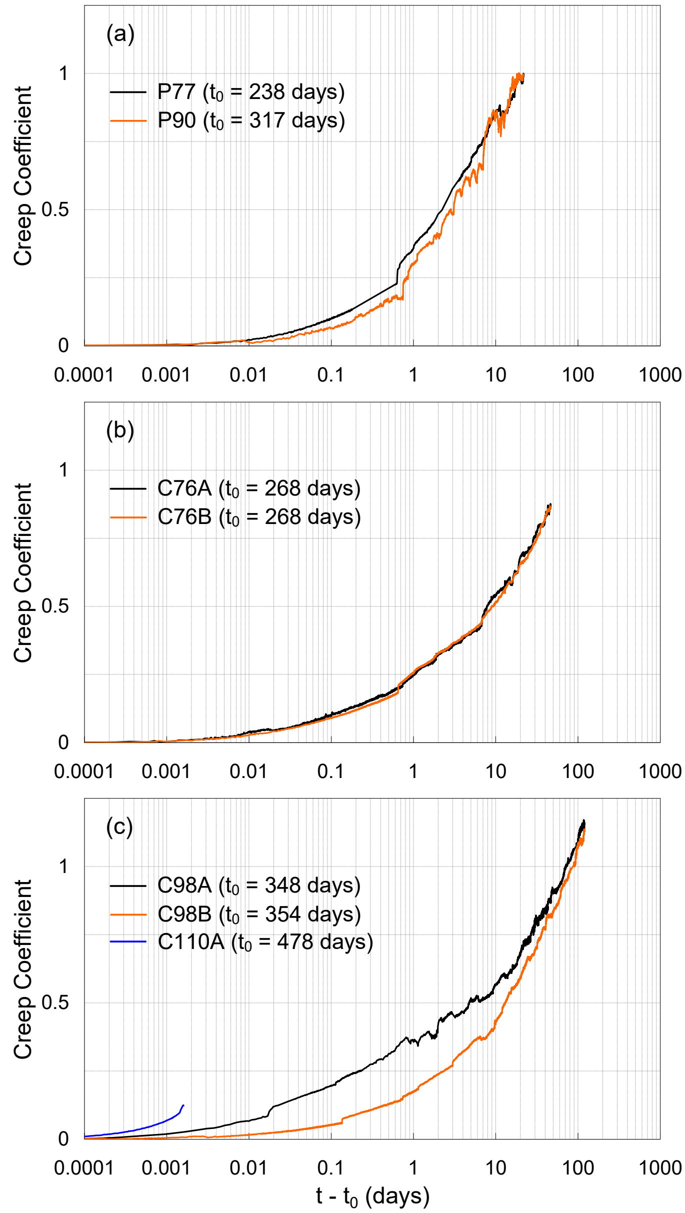

Fig. 7. Creep coefficient during sustained concentric loading.

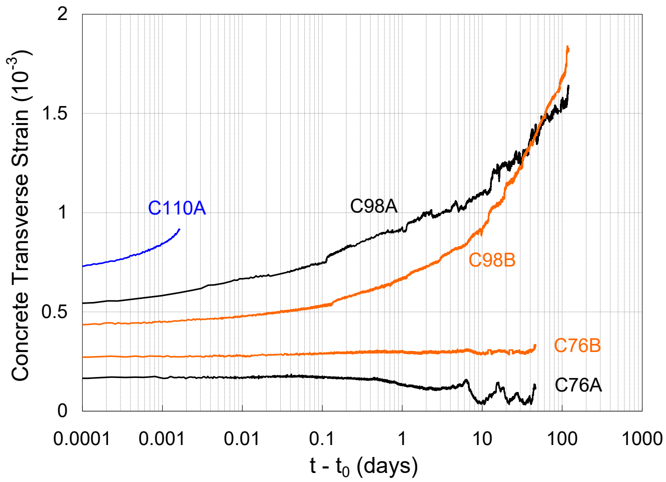

Fig. 8. Transverse strain of concrete cover during sustained concentric loading.

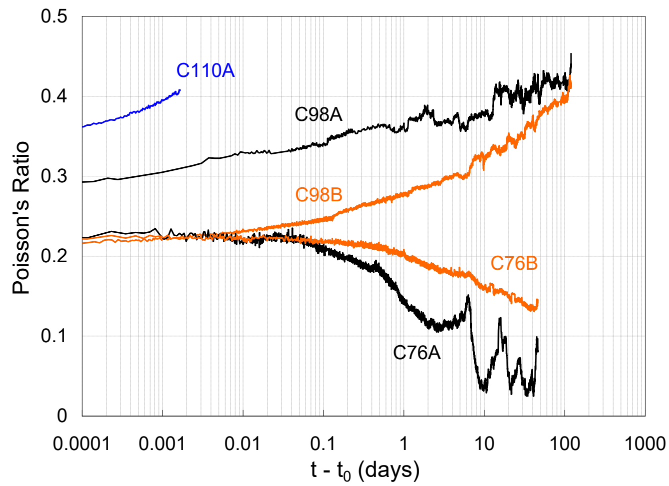

Fig. 9. Variation of Poisson’s ratio during sustained concentric loading.

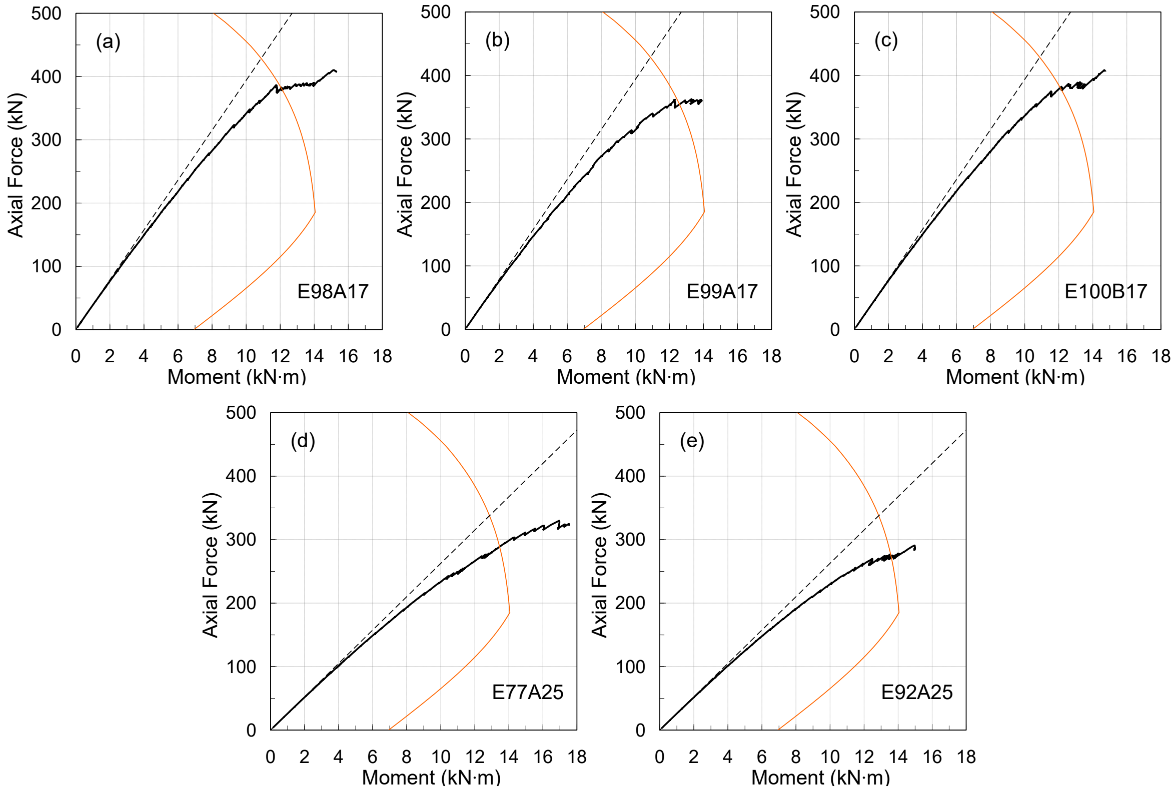

Fig. 10. Load-moment response at column mid-height.

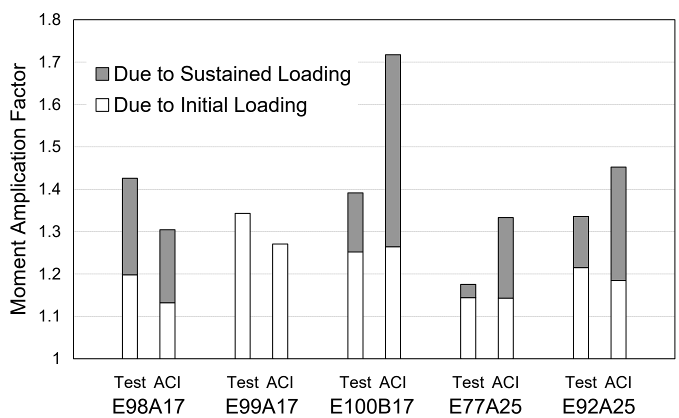

Fig. 11. Comparison of moment amplification factors obtained from tests and ACI 318 formulations.

E98A17 E99A17 E100B17 E77A25 E92A25

Fig. 12. Damage and failure mode of eccentrically loaded columns.

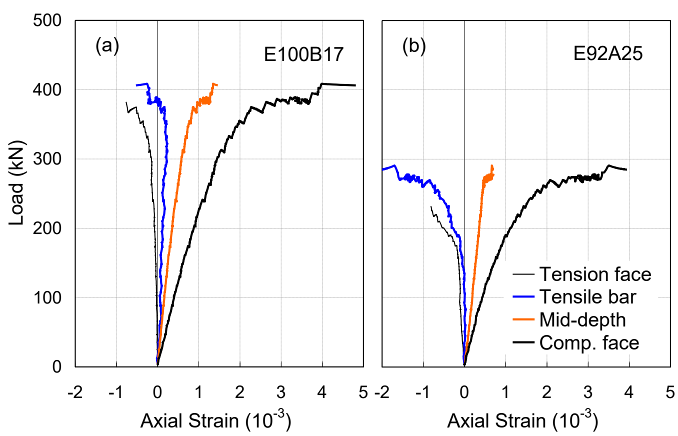

Fig. 13. Axial strains at four locations in Specimens E100B17 and E92A25.

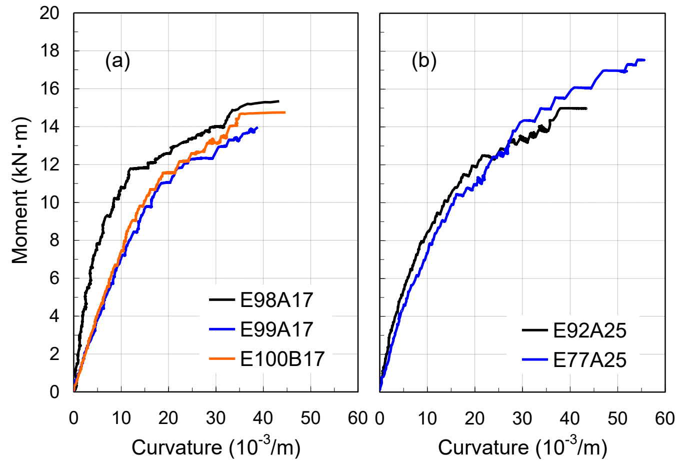

Fig. 14. Moment-curvature response of columns under eccentric loading: (a) $e/h = 0.17$; (b) $e/h = 0.25$. eccentric loading.

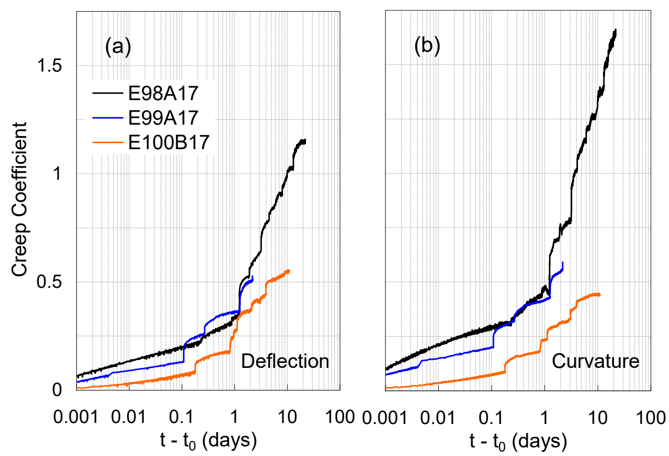

Fig. 15. Creep coefficient of columns ($e/h = 0.17$) at mid-height: (a) deflection; (b) curvature.

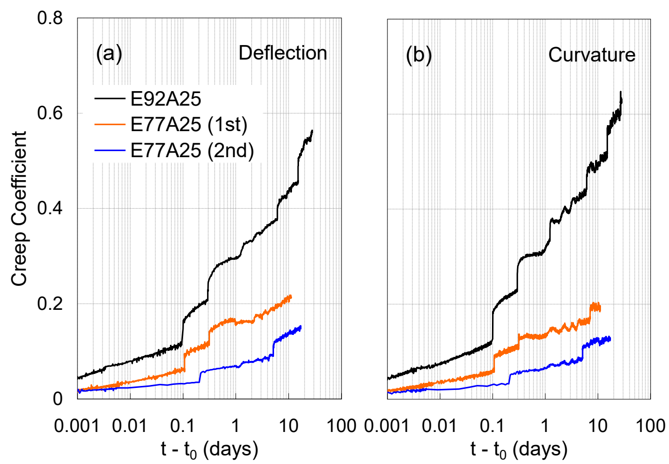

Fig. 16. Creep coefficient of columns ($e/h = 0.25$) at mid-height: (a) deflection; (b) curvature.

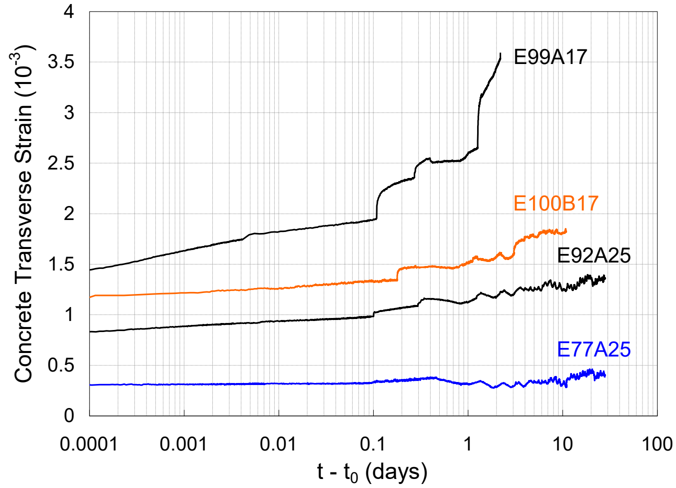

Fig. 17. Transverse strain of concrete cover at compression side during sustained eccentric loading.

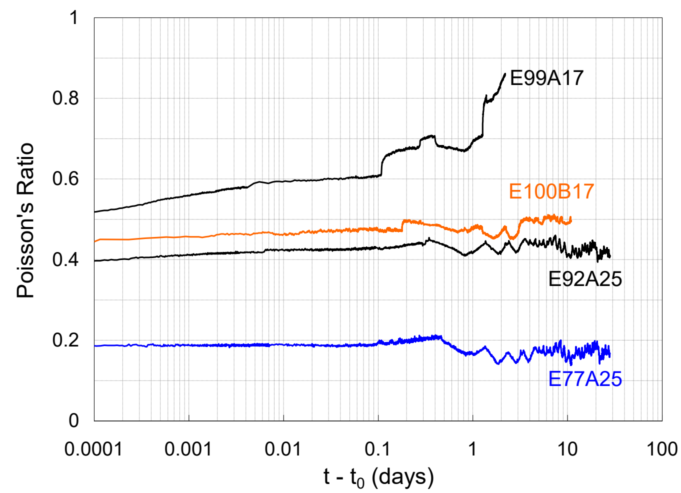

Fig. 18. Poisson's ratio of concrete cover at compression side during sustained eccentric loading.